3-D Measurement of Objects in a Cylindrical Glass Water Tank with a Laser Range Finder

Atushi Yamashita[†], Etsukazu Hayashimoto[†,‡], Toru Kaneko[†] and Yoshimasa Kawata[†]
[†] Department of Mechanical Engineering, Shizuoka University
3-5-1 Hamamatsu-shi, Shizuoka 432-8561, Japan
[‡] Pulstec Industrial Co., Ltd.
E-mail address: yamashita@ieee.org

***Abstract*— In this paper, we propose a three-dimensional (3-D) measurement method of objects in liquid with a laser range finder. When applying vision sensors to measuring objects in liquid, we meet the problem of an image distortion. It is caused by the refraction of the light on the boundary between the air and the liquid, and the distorted image brings errors in a triangulation for the range measurement. Our proposed method can measure the accurate 3-D coordinates of object surfaces in liquid taken for calculating the refraction effect. The effectiveness of the proposed technique is shown through experiments. The accuracy of the 3-D measurement is 0.7mm for objects located about 250mm from the laser range finder when considering the refraction of the light, although that is 2.9mm without the consideration of it.**

key words: three-dimensional measurement, refraction, objects in liquid, triangulation, laser range finder

I. INTRODUCTION

Acquisition of three-dimensional (3-D) coordinates of object surfaces is required in many applications. Especially, optical measurement is preferred as a non-contact method, and much effort has been made on developing vision sensor systems with optical sensors and digital processors based on the triangulation range sensing [1]. However, they have been almost applied to the measurement of objects in aerial or outer-space environments, and little consideration has been made on the application to the measurement of objects in liquid. In the latter case, acoustical methods using sonar are often used [2], [3], especially for underwater robots [4], [5]. However, they do not give high resolution due to relatively longer wavelength of ultrasonic waves than that of the light. Therefore, the photogrammetric images are effective for the 3-D measurement [6], [7].

When applying vision sensors to measuring objects in liquid, we meet the problem of the image distortion. It is caused by the refraction on the boundary between the air and the liquid, and the distorted image brings errors in the triangulation for the range measurement. Figure 1 shows an example of the distorted image that single rectangular object is in a cylindrical glass water tank. The edge of the object on the boundary between the air and the liquid looks discontinuous and it appears to that two objects exist.

Fig. 1. Example of image distortion.

The problem occurs not only when a vision sensor is set outside the liquid but also when it is set inside, because in the latter case we should usually place a protecting glass plate in front of viewing lens or a laser beam scanner.

Therefore, 3-D measurement methods for these cases are proposed [7], [8]. However, the methods by using a stereo camera system have the problem that the corresponding points are difficult to detect when the texture of the object's surface is simple in particular when there is the refraction on the boundary between the air and the liquid [7]. The methods by using a laser range finder are also proposed for the detection of the corresponding points [8], however, these methods can only treat with the situation that the shape of the boundary between the air and the liquid is flat.

In this paper, we propose a 3-D measurement method of objects in liquid by using a laser range finder to handle the cases that the shape of the refraction boundary is not flat. The 3-D coordinates of object surfaces are measured by the camera and the spot laser beam that can change its direction upward and downward (Fig. 2). We adopt a cylindrical beaker filled with the water as the arbitrary glass water tank whose shape is not flat. The water tank is set on the turntable and object shape is measured while rotating the turntable.

Our proposed method can be used for the measurement of objects that cannot be contacted such as the very important samples like creatures that are pickled in formalin. This method also can be applied to the measurement

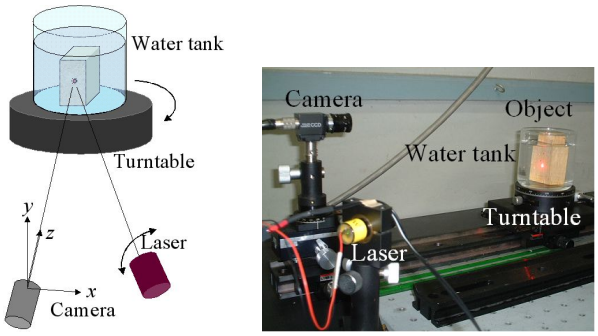

(a) Schematic. (b) Experimental equipment.

Fig. 2. Overview of 3-D measurement.

of objects in various water tank, and the underwater observation by underwater robots.

The composition of this paper is detailed below. In Section 2, the principle of the 3-D measurement is explained. In this section, the explanation is for a cylindrical shape that has a taper. Our method can also treat arbitrary-shaped boundaries of the refraction because we consider the 3-D model of the refraction in this paper. In Section 3, the process of the 3-D measurement of objects is constructed. In Section 4, we verify our method with experiments and Section 5 describes conclusions.

II. PRINCIPLE OF 3-D MEASUREMENT

The principle of the 3-D measurement is based on a 3-D optical ray tracing technique that properly models the situation. The ray from the camera and that from the laser are traced respectively and the intersection point of two rays corresponds to the surface of the object.

Figure 3 shows the model of the optical rays. Here, let $C_0 : (x_{c0}, y_{c0}, z_{c0})^T$ be the center of the camera lens, $O : (x_O, y_O, z_O)^T$ be the centroid of the water tank (y_O means the height of the centroid axis), $L_0 : (x_{l0}, y_{l0}, z_{l0})^T$ be the starting point of the laser beam, and $\vec{d}_{l1} = (\alpha_{l1}, \beta_{l1}, \gamma_{l1})^T$ be the unit vector of the laser beam. These parameters can be calibrated in advance.

A. Ray Tracing from Camera

In this model, a pinhole camera model is adopted. The coordinate $(u,v)^T$ on the image plane is translated to the coordinate $(x,y,z)^T$ on the world coordinate.

$$\begin{pmatrix} x \\ y \\ z \end{pmatrix} = \begin{pmatrix} a_{11} & a_{12} & a_{13} \\ a_{21} & a_{22} & a_{23} \\ 0 & 0 & f \end{pmatrix} \begin{pmatrix} u \\ v \\ 1 \end{pmatrix}, \tag{1}$$

where f is the image distance[1], and a_{ij} is the other camera parameters. The direction vector of the ray from the camera is expressed as:

[1]The image distance is equal to the distance between the center of lens and the image plane. Although it is confusable, the image distance is not same as the focal length. When an image of an infinitely (or at least sufficiently) distant object is created on the sensor, this distance is equal to the focal length of the lens [9].

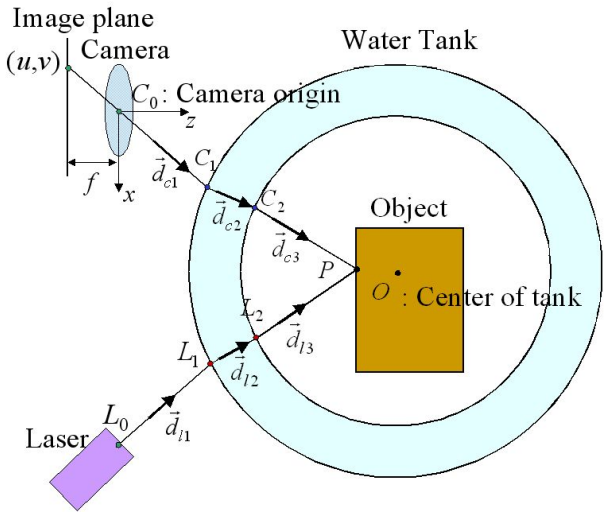

Fig. 3. Principle of 3-D measurement.

$$\begin{pmatrix} \alpha_{c1} \\ \beta_{c1} \\ \gamma_{c1} \end{pmatrix} = \frac{1}{\sqrt{x^2+y^2+f^2}} \begin{pmatrix} x \\ y \\ f \end{pmatrix}. \tag{2}$$

After that, $C_1 : (x_{c1}, y_{c1}, z_{c1})^T$ (the intersection point between the ray $\vec{d}_{c1}$ from the camera and the outside surface of the water tank) is obtained by using the distance ρ_{c1} between the camera and the outside surface of the water tank.

$$\begin{pmatrix} x_{c1} \\ y_{c1} \\ z_{c1} \end{pmatrix} = \rho_{c1} \begin{pmatrix} \alpha_{c1} \\ \beta_{c1} \\ \gamma_{c1} \end{pmatrix} + \begin{pmatrix} x_{c0} \\ y_{c0} \\ z_{c0} \end{pmatrix}. \tag{3}$$

When R_0 is the radius of the water tank bottom and ϕ_1 is the taper angle of the water tank, the unit normal vector of the water tank surface $\vec{N}_{c1} = (\lambda_{c1}, \mu_{c1}, \nu_{c1})^T$ at the C_1 is calculated as follows:

$$\begin{pmatrix} \lambda_{c1} \\ \mu_{c1} \\ \nu_{c1} \end{pmatrix} = m_1 \begin{pmatrix} x_O - x_{c1} \\ y_O - y_{c1} \\ z_O - z_{c1} \end{pmatrix}, \tag{4}$$

where

$$m_1 = \frac{\cos\phi_1}{R_0 - (\rho_{c1}\beta_{c1} + y_{c0})\tan\phi_1}, \tag{5}$$

$$\mu_{c1} = -\sin\lambda_{c1}. \tag{6}$$

Because N_{c1} is a normal vector, the following equation is gained:

$$\lambda_{c1}^2 + \mu_{c1}^2 + \nu_{c1}^2 = 1. \tag{7}$$

From (2)–(7), ρ_{c1} can be obtained in (8), and the coordinate values of C_1 is decided.

$$\rho_{c1} = \frac{\rho_{c1b} - \sqrt{\rho_{c1b}^2 - \rho_{c1a}\rho_{c1c}}}{\rho_{c1a}}, \tag{8}$$

where

$$\rho_{c1a} = \alpha_{c1}^2 - \beta_{c1}^2 \tan^2\phi_1 + \gamma_{c1}^2, \quad (9)$$

$$\rho_{c1b} = \alpha_{c1}(x_O - x_{c0}) - \beta_{c1}\tan\phi_1(R_0 - y_{c0}\tan\phi_1) + \gamma_{c1}(z_O - z_{c0}), \quad (10)$$

$$\rho_{c1c} = (x_O - x_{c0})^2 + (R_0 - y_{c0}\tan\phi_1)^2 + (z_O - z_{c0})^2. \quad (11)$$

Next, the ray between the outside and the inside of the water tank can be traced. The unit vector of the ray $\vec{d}_{c2} = (\alpha_{c2}, \beta_{c2}, \gamma_{c2})^T$ from C_1 is expressed as the linear sum of $\vec{d}_{c1}$ and $\vec{N}_{c1}$ because these three vectors are on the same plane.

$$\begin{pmatrix} \alpha_{c2} \\ \beta_{c2} \\ \gamma_{c2} \end{pmatrix} = p_{c1} \begin{pmatrix} \alpha_{c1} \\ \beta_{c1} \\ \gamma_{c1} \end{pmatrix} + q_{c1} \begin{pmatrix} \lambda_{c1} \\ \mu_{c1} \\ \nu_{c1} \end{pmatrix}, \quad (12)$$

where p_{c1} and q_{c1} are the constants.

Here, let θ_{c1} be the angle of incident (the angle between $\vec{d}_{c1}$ and $\vec{N}_{c1}$), and θ_{c2} be the angle of refraction (the angle between $\vec{d}_{c2}$ and $-\vec{N}_{c1}$). The inner product of $\vec{d}_{c1}$ and $\vec{N}_{c1}$ is calculated as:

$$\vec{d}_{c1} \cdot \vec{N}_{c1} = \alpha_{c1}\lambda_{c1} + \beta_{c1}\mu_{c1} + \gamma_{c1}\nu_{c1} = \cos\theta_{c1}. \quad (13)$$

The outer product is also calculated.

$$|\vec{d}_{c1} \times \vec{N}_{c1}|^2 = (\beta_{c1}\nu_{c1} - \gamma_{c1}\mu_{c1})^2 + (\gamma_{c1}\lambda_{c1} - \alpha_{c1}\nu_{c1})^2 + (\alpha_{c1}\mu_{c1} - \beta_{c1}\lambda_{c1})^2 = \sin^2\theta_{c1}. \quad (14)$$

About $\vec{d}_{c2}$ and $-\vec{N}_{c1}$, the inner and the outer products can be calculated in the same way.

$$\cos\theta_{c2} = \alpha_{c2}\lambda_{c1} + \beta_{c2}\mu_{c1} + \gamma_{c2}\nu_{c1}, \quad (15)$$

$$\sin^2\theta_{c2} = (\beta_{c2}\nu_{c1} - \gamma_{c2}\mu_{c1})^2 + (\gamma_{c2}\lambda_{c1} - \alpha_{c2}\nu_{c1})^2 + (\alpha_{c2}\mu_{c1} - \beta_{c2}\lambda_{c1})^2. \quad (16)$$

Incidentally, the Snell's low of the refraction is also applied at the point C_1:

$$\frac{n_1}{n_2} = \frac{\sin\theta_{c2}}{\sin\theta_{c1}}, \quad (17)$$

where n_1 and n_2 are the refraction index before and after the point C_1, respectively (n_1: the refraction index of the air, n_2: that of the glass).

From (12)–(17), p_{c1} and q_{c1} are obtained as:

$$p_{c1} = \frac{n_1}{n_2}, \quad (18)$$

$$q_{c1} = \sqrt{1 - \left(\frac{n_1}{n_2}\right)^2 \sin^2\theta_{c1}} - \frac{n_1}{n_2}\cos\theta_{c1}. \quad (19)$$

In the same way of calculating C_1, the coordinate values of C_2 (the intersection point between the ray from C_1 and the inside surface of the water tank) are also obtained. After that, the refraction at the point C_2 can be considered. A unit vector of the ray from C_2 is obtained as follows when n_3 is the refraction index after the point C_2 (the refraction index of the liquid in the water tank).

$$\begin{pmatrix} \alpha_{c3} \\ \beta_{c3} \\ \gamma_{c3} \end{pmatrix} = p_{c2} \begin{pmatrix} \alpha_{c2} \\ \beta_{c2} \\ \gamma_{c2} \end{pmatrix} + q_{c2} \begin{pmatrix} \lambda_{c2} \\ \mu_{c2} \\ \nu_{c2} \end{pmatrix}, \quad (20)$$

where

$$p_{c2} = \frac{n_2}{n_3}, \quad (21)$$

$$q_{c2} = \sqrt{1 - \left(\frac{n_2}{n_3}\right)^2 \sin^2\theta_{c2}} - \frac{n_2}{n_3}\cos\theta_{c2}. \quad (22)$$

The ray from the camera finally reaches on the surface of the object at the point $P_c : (x_{pc}, y_{pc}, z_{pc})^T$.

$$\begin{pmatrix} x_{pc} \\ y_{pc} \\ z_{pc} \end{pmatrix} = c \begin{pmatrix} \alpha_{c3} \\ \beta_{c3} \\ \gamma_{c3} \end{pmatrix} + \begin{pmatrix} x_{c2} \\ y_{c2} \\ z_{c2} \end{pmatrix}, \quad (23)$$

where $(x_{c2}, y_{c2}, z_{c2})^T$ is the coordinate values at the point C_2, $\vec{d}_{c3} = (\alpha_{c3}, \beta_{c3}, \gamma_{c3})^T$ is the ray from the point C_2, and c is a constant. The 3-D coordinate values at P_c is obtained when c are gained.

B. Ray Tracing from Laser

The ray tracing from the starting point of the laser can be executed in the same way of the camera. Finally, the ray from the laser reaches on the surface of the object at the point $P_l : (x_{pl}, y_{pl}, z_{pl})^T$.

$$\begin{pmatrix} x_{pl} \\ y_{pl} \\ z_{pl} \end{pmatrix} = l \begin{pmatrix} \alpha_{l3} \\ \beta_{l3} \\ \gamma_{l3} \end{pmatrix} + \begin{pmatrix} x_{l2} \\ y_{l2} \\ z_{l2} \end{pmatrix}, \quad (24)$$

where $(x_{l2}, y_{l2}, z_{l2})^T$ is the coordinate values at the point L_2, $\vec{d}_{l3} = (\alpha_{l3}, \beta_{l3}, \gamma_{l3})^T$ is the ray from the point L_2, and l is a constant.

C. Determination of 3-D Coordinate Value

The point on the surface of the object coincides both P_c and P_l. Therefore, we can obtain c and l by considering (23) and (24) as the simultaneous equations that $(x_{pc}, y_{pc}, z_{pc})^T = (x_{pl}, y_{pl}, z_{pl})^T$. However, these three equations cannot be satisfied at the same time. This is because the number of unknown parameters is two (c and l), and the number of the equations is three (x, y, and z coordinate values). It occurs when there are errors of the parameters obtained from the calibration and those of the image processing when measuring.

Therefore, we regard the middle point of two rays (from the camera and the laser) as the surface of the object where

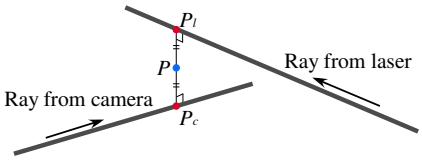

Fig. 4. Determination of 3-D position of P.

the distance between two rays becomes the shortest (Fig. 4).

The optimal value of parameter l when two rays approach most is obtained as follows:

$$l = \frac{L_a}{\cos^2\theta_p - 1}, \tag{25}$$

where

$$\begin{aligned} \cos\theta_p &= \alpha_{c3}\alpha_{l3} + \beta_{c3}\beta_{l3} + \gamma_{c3}\gamma_{l3}, & (26)\\ L_a &= (\alpha_{l3} - \alpha_{c3}\cos\theta_p)(x_{l2} - x_{c2}) \\ &\quad +(\beta_{l3} - \beta_{c3}\cos\theta_p)(y_{l2} - y_{c2}) \\ &\quad +(\gamma_{l3} - \gamma_{c3}\cos\theta_p)(z_{l2} - z_{c2}). & (27) \end{aligned}$$

Therefore, P_l can be calculed in (24). In the same way, parameter c and P_c can be also calculated.

Conclusively, the surface of the object $P : (x_p, y_p, z_p)^T$ is obtained.

$$\begin{pmatrix} x_p \\ y_p \\ z_p \end{pmatrix} = \frac{1}{2}\begin{pmatrix} x_{pc} + x_{pl} \\ y_{pc} + y_{pl} \\ z_{pc} + z_{pl} \end{pmatrix}. \tag{28}$$

III. PROCEDURE OF 3-D MEASUREMENT

A. Calibration of Equipment

We must calibrate the camera parameters, the starting point and the direction vector of the laser beam, the center of the rotation of the turntable, and the centroid of the water tank for measuring the 3-D coordinate values of the object in liquid.

At first, the camera parameters are calibrated by using the planner pattern on which surface checked patterns are drawn.

Next, the starting point L_0 and the direction vector of the laser beam $\vec{d}_{l1}$ are calibrated by changing the direction of the laser and the position of the planner pattern.

After that, the center of the rotation of the turntable is calibrated by using the object whose shape is known on the turntable (Fig. 5(a)). The rotational center of the turntable is estimated by the exploratory search. The difference between the known shape and the result of the reconstructed shape with the 3-D measurement by using our calibrated laser range finder is minimized to obtain the position of the rotational center.

Finally, the relationship between the centroid of the water tank and the rotational center of the turntable is estimated. It is realized by applying the non-transparent

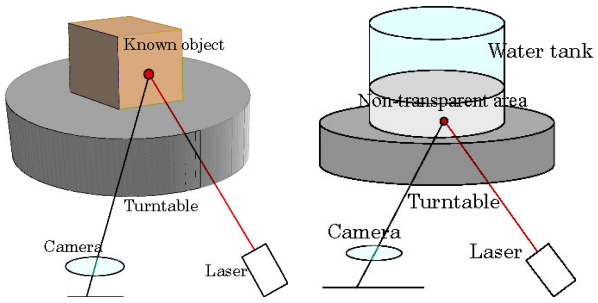

(a) Rotational center. (b) Centroid of tank.

Fig. 5. Calibration method.

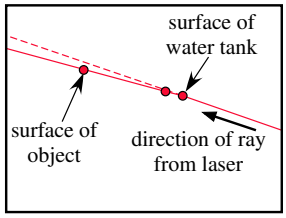

Fig. 6. Extraction of laser point.

sheet on the surface of the water tank (Fig. 5(b)). The areas where the sheets attach block the laser beam. The accurate 3-D coordinate values of the water tank surface can be measured in these areas. From these result, we can obtain the position of its centroid.

B. 3-D Shape Measurement

After all the calibration, 3-D shape measurement of objects in liquid is executed. The images are acquired while the turntable is rotating. After going into a 360-degree roll, the angle of the laser beam changes to measure the shape of another cross-sectional surface.

C. Extraction of Laser Points on Object

About the extraction of the spot light of the laser in the acquired images, the epipolar constraints and the subpixel calculation are utilized.

Rough areas of the laser beam in the images are limited by the epipolar constraints. When multiple points are detected as the laser light, we can judge the point on the surface of the object that the objective point exists in the deepest direction of the epipolar line in any cases (Fig. 6).

The subpixel measurement is executed by calculating the center of gravity of the extracted pixels that belong to the laser light as follows:

$$\begin{pmatrix} u_g \\ v_g \end{pmatrix} = \frac{1}{\sum t(u_i, v_i)}\begin{pmatrix} \sum t(u_i, v_i)u_i \\ \sum t(u_i, v_i)v_i \end{pmatrix}, \tag{29}$$

where $t(u_i, v_i)$ $(> T)$ is the pixel value at the i-th pixel (u_i, v_i) that belongs to the laser light, and (u_g, v_g) is the position of subpixel order on which the laser beam illuminates (T: a threshold value given in advance).

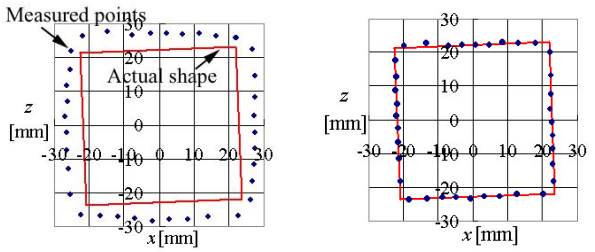

(a) Before calibration. (b) After calibration.

Fig. 7. Calibration results of rotational center.

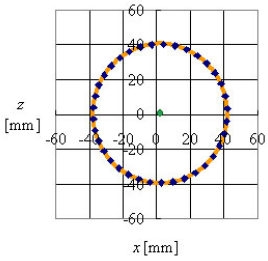

Fig. 8. Calibration results of water tank centroid.

IV. EXPERIMENTS

We use a cylindrical glass water tank whose inside radius of the bottom is 38.2mm and outside radius is 39.9mm. The tank is filled with the water. The refraction index of the air (n_1), the glass (n_2), and the water (n_3) is as follows: $n_1 = 1.000$, $n_2 = 1.5000$, $n_3 = 1.335$. The resolution of images is 640 $\times$ 480pixel. The camera parameter f is estimated as 1085.0pixel from the camera calibration.

The calibration of the rotational center of the turntable is executed by using the rectangular object whose cross-section shape is 44.5mm $\times$ 45.1mm. Figure 7 shows the results before and after the calibration. The coordinate value of the rotational center before the calibration is $(0.00, 0.00, 250.00)^T$, and that after it is $(1.23, 0.00, 239.24)^T$ in this case. In Fig. 7, (blue) points are the measured 3-D positions and (red) lines are the actual shapes of the object. The average distance between the measured points and the actual lines is about 0.10mm after the calibration of the rotational center.

Figure 8 shows the results of the estimation of the centroid of the water tank. The coordinate value of the centroid of the water tank is estimated as $(3.42, 0.00, 239.74)^T$ in this case. The distance between the measured points and the circle that indicates the real shape of the water tank becomes very small after the calibration of the centroid.

Experiments are done by using the object whose cross-section shape is 33.5mm $\times$ 22.5mm under the various situations. The turntable is rotated in 10deg interval.

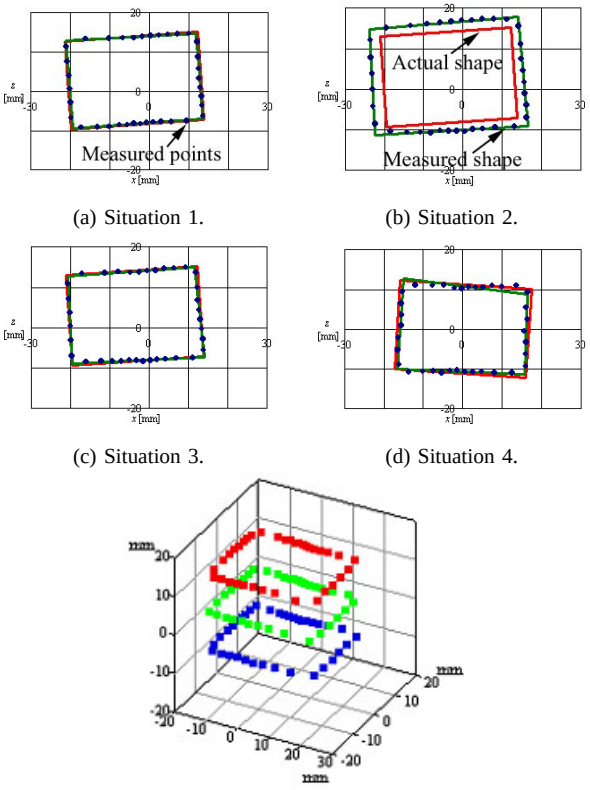

(a) Situation 1. (b) Situation 2.

(c) Situation 3. (d) Situation 4.

(e) Result of 3-D shape measurement.

Fig. 9. Experimental results I.

TABLE I

RESULTS OF THE LEAST SQUARE ESTIMATION.

Situation	Standard deviation	Maximum error
1	0.10mm	0.26mm
2	0.18mm	0.58mm
3	0.14mm	0.31mm
4	0.55mm	1.80mm

1) 3-D measurement of the object in the water tank **without** the water. The distance between the object and the laser range finder is 239.24mm (Fig. 9(a)).
2) 3-D measurement of the object in the water tank **filled with** the water and **without** the consideration of the refraction of the light. The distance is 239.24mm (Fig. 9(b)).
3) 3-D measurement of the object in the water tank **filled with** the water and **with** the consideration of the refraction. The distance is 239.24mm (Fig. 9(c)).
4) 3-D measurement of the object in the water tank **filled with** the water and **with** the consideration of the refraction. The distance is **500.37mm** (Fig. 9(d)).

The results of these situations are shown in Fig. 9(a)–(d), and the quantitative results are shown in Table I and Table II.

TABLE II

DIFFERENCE BETWEEN REAL SHAPE AND MEASURED POINTS.

Situation	Average error	Maximum error
1	0.23mm	0.42mm
2	2.26mm	2.93mm
3	0.31mm	0.72mm
4	0.73mm	1.21mm

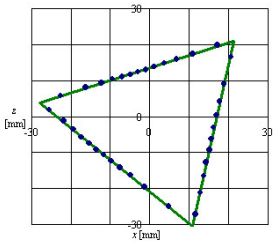

Fig. 10. Experimental results II.

In Fig. 9(a)–(d), (blue) points indicate the measured positions, (green) deep lines indicate the lines by the least square estimation from the measured positions, and (red) thin lines indicate the actual shapes of the object.

Table I indicates the standard deviations and the maximum errors between the lines of the least square estimation and the actual measured points. This result predicates the fitting accuracy of each lines of the object surface. Table II indicates the difference between the real shape of the object and the actual measured points. This result indicates the accuracy of the 3-D measurement in totality.

From the result of Situation 1, the accuracy of the calibration is verified because the measured shape of the object is almost same with the actual one.

When the result of Situation 3 is compared with that of Situation 2 in Table II, the accuracy is improved dramatically. The accuracy when water exists is almost same with that when water does not exist. Therefore, it is found out that the consideration of the refraction of the light is very important and effective when objects in liquid are measured.

The result of Situation 4 shows the accuracy of the 3-D measurement depends on the distance between the laser range finder and the object.

In these experiments, the accuracy of all the results by using our proposed method is within the subpixel order.

The result of the 3-D measurement when the distance between the object and the laser range finder is 239.24mm is shown in Fig. 9(e). From this result, it is verified that the measurement about the height direction is also performed correctly. The measurement result of another shape object is shown in Fig. 10. These results show that our method can work without failure regardless of the shape of the object and the direction of the laser beam.

V. CONCLUSIONS

In this paper, we propose a 3-D measurement method of objects in liquid with a laser range finder. We take the refraction of the light into consideration in the triangulation, and build the technique that is suitable for objects in liquid. Experiments have verified the effectiveness of proposed 3-D measurement method. The accuracy of the results is within subpixel order of acquired images.

As the future works, it is desirable that the refraction index, the shape of the water tank, and the shape of the object inside the tank are measured simultaneously. The wide range shape of the object must be also measured by using the slit light of the laser in place of the spot light.

VI. ACKNOWLEDGMENTS

This research was partially supported by the Ministry of Education, Culture, Sports, Science and Technology, Grant-in-Aid for Scientific Research (C), 14550416, 2002.

VII. REFERENCES

[1] D. Nitzan: “Three-Dimensional Vision Structure for Robot Applications,” *IEEE Transactions on Pattern Recognition and Machine Intelligence*, Vol.10, No.3, pp.291–309, 1988.

[2] B. Kamgar-Parsi, L. J. Rosenblum and E. O. Belcher: “Underwater Imaging with a Moving Acoustic Lens,” *IEEE Transactions on Image Processing*, Vol.7, No.1, pp.91–99, 1998.

[3] V. Murino, A. Trucco and C. S. Regazzoni: “A Probalilistic Approach to the Coupled Reconstruction and Restortion of Underwater Acoustic Images,” *IEEE Transactions on Pattern Analysis and Machine Intelligence*, Vol.20, No.1, pp.9–22, 1998.

[4] J. S. Jaffe: “Computer Modeling and the Design of Optimal Underwater Imaging Systems,” *IEEE Journal of Oceanic Engineering*, Vol.15, No.2, pp.101–111, 1990.

[5] J. Yuh and M. West: “Underwater Robotics,” *Advanced Robotics*, Vol.15, No.5, pp.609–639, 2001.

[6] R. F. Tusting and D. L. Davis: “Laser Systems and Structured Illumination for Quantitative Undersea Imaging,” *Marine Technology Society Journal*, Vol.26, No.4, pp.5–12, 1992.

[7] R. Li, H. Li, W. Zou, R. G. Smith and T. A. Curran: “Quantitive Photogrammetric Analysis of Digital Underwater Video Imagery,” *IEEE Journal of Oceanic Engineering*, Vol.22, No.2, pp.364–375, 1997.

[8] T. Kaneko, D. Nakayama and T. Kubo: “Determination of Observing Optical Geometry for Three-Dimensional Measurement of Objects in Liquid,” *Proceedings of Optics in Computing*, pp.453–456, 1998.

[9] S. G. Lipson, H. Lipson and D. S. Tannhauser: *Optical Physics Third Edition*, Cambridge University Press, 1995.